Desalination and Water Treatment
www.deswater.com

doi: 10.5004/dwt.2022.28016

246 (2022) 156–165
January

Electrically conductive membrane of polycarbazole Sn(IV) phosphate cation exchange nanocomposite and their ion-selective and sorption studies

Mohd. Zeeshan[a,*], Rais Ahmad[a], Asif Ali Khan[a], Aftab Aslam Parwaz Khan[b,c], Hadi M. Marwani[b,c], Mohamed Shaban[d], Abdullah M. Asiri[b,c], Sakshi Singh[e]

[a]*Department of Applied Chemistry, F/O Engineering and Technology, Aligarh Muslim University, Aligarh 202002, India, emails: mohd.zee2010@gmail.com (M. Zeeshan), rais45@rediffmail.com (R. Ahmad), asifkhan42003@yahoo.com (A.A. Khan)*
[b]*Center of Excellence for Advanced Materials Research, King Abdulaziz University, Jeddah 21589, Saudi Arabia*
[c]*Chemistry Department, King Abdulaziz University, Faculty of Science, Jeddah 21589, Saudi Arabia, emails: draapk@gmail.com (A.A.P. Khan), hmarwani@kau.edu.sa (H.M. Marwani), aasiri2@gmail.com (A.M. Asiri)*
[d]*Nanophotonics and Applications Lab, Physics Department, Faculty of Science, Beni-Suef University, Beni-Suef 62514, Egypt, email: mssfadel@aucegypt.edu (M. Shaban)*
[e]*Department of Basic Science and Humanities, Oriental University Indore, emails: singh.sakshi3354@gmail.com (S. Singh)*

Received 17 March 2021; Accepted 18 November 2021

ABSTRACT

This work presents a novel organic–inorganic nanocomposite ion exchanger synthesized through an in-situ approach that exhibits exceptional ion exchange capacities (IEC~1.95 meq g^{-1}). Through solution casting, polycarbazole (PCz) Sn(IV) phosphate ion-exchange membranes were also prepared. Several instruments were utilized to characterize membranes including scanning electron microscopy with thermogravimetric analysis, Fourier-transform infrared spectroscopy, X-ray diffraction, transmission electron microscopy, and energy-dispersive X-ray spectroscopy. A few parameters, including the working pH range (5–8), the response time (20 s), the linear response range (1.0×10^{-7} M to 1.0×10^{-1} M), and the detection limit (1.0×10^{-7} M), were measured following fabrication of Cu^{2+} selective membrane electrodes. It also serves as an indicator electrode during the Cu^{2+} potentiometric titration.

Keywords: Nanocomposites; Electroactive material; Ion-exchange membrane; Ion-selective electrode

1. Introduction

Ion-exchange materials have emerged to be the latest area of interest during the last decade within the scientific community which owes to their unique chemical, magnetic, optical, and electrical properties. These techniques can be applied to electroanalytical [1], catalysis, water treatment processes [2], and various other fields [3,4]. The ion exchangers' efficiency can be enhanced considerably through carrying out the commercially accessible ion exchange polymeric materials' desired modification using various techniques. A metal nanoparticle is used in the present study for improving the properties of the ion exchanger [5]. Synthesis of the metal nanoparticles is carried out by uses of in-situ oxidative synthesis techniques (IMS) [6]. These materials comprise of nanometer-sized metallic clusters, surface protrusions materials separated via nanometric distance, polycrystalline materials (with nanometer-sized crystallites), or porous material (with nanometer range porous size) [7]. In recent times, in the cations' determination and detection, organic-inorganic composite ion exchanger materials have been employed

* Corresponding author.

effectively by effecting their ion-selective membrane electrode [8–10]. The use of membranes for the separation of substances has been of utmost importance in both industrial as well as biological processes. In aqueous solution ionic groups having electrolytes permeable ion-exchange membranes are greatly utilized in various area such as analytical chemistry, batteries' solid polymer electrolyte, dialysis, etc. [11,12]. Nowadays, Nafion is one of the most popular and effective ion-exchange membranes. Applied as a conductive binder etc. The combination of all these properties makes it ideal for analytical applications [13–20].

Environment monitoring using selective ion-exchange membranes is the need of the hour for water purification and vapor sensing. Some ion-exchange membranes selective for Pb^{2+}, Hg^{2+}, Cd^{2+}, Ni^{2+} have been reported previously [8,9,21–24].

In this research, work efforts were performed for preparing Cu^{2+} sensitive membrane electrode by utilizing PCz-Sn(IV)phosphate nanocomposite cation exchanger and apply it in electroanalytical studies.

2. Experimental

2.1. Chemicals, reagents and instruments

For the synthesis primary reagent utilized are; carbazole monomer, and iron(III)chloride (98%) were obtained from Merck, Germany. HCl (35%) and chloroform ($CHCl_3$) were obtained from Rainchem; orthophosphoric acid (H_3PO_4) from Thomas Baker; and copper nitrate ($Cu(NO_3)_2$) from E-Merck (India Ltd.). Every reagent as well as chemicals utilized of analytical reagent grade. Demineralized water (DMW) was utilized for all the solutions and all practical purposes preparation during the experiments. For morphological and structural characterization, below instruments were utilized: "1148/89 based diffractometer with Cu Ka radiations, TGA (thermogravimetric analysis) utilizing Rigaku X-ray powder diffractometer and thermal analyzer-V2.2A DuPont 9900 with Cu anode (Kα λ = 1.54186 Å) utilzing a PW, EDX (energy-dispersive X-ray spectroscopy) and SEM (scanning electron microscopy) (LEO 435-VF), Fourier-transform infrared (FTIR) spectrophotometer (Perkin-Elmer, USA, model Spectrum-BX, range 4,000–400 nm). Furthermore, as reference electrode, having 1 mV accuracy, digital potentiometer (Equiptronics EQ 609, India) with a saturated calomel electrode" was utilized for analytical studies.

2.2. Synthesis of Sn(IV)phosphate inorganic precipitate

Sn(IV)phosphate was formulated by combining 0.1 M orthophosphoric acid and 0.1 M stannic chloride (prepared in 1 M HCl) at room temperature (25°C ± 2°C). Solution's pH is maintained at 1 through constant stirring. Sn(IV)arsenotungstate's white colored gel was acquired which was then for 24 h is permitted to settle. Then, it was washed and filtered under DMW suction till neutral pH is presented by filtrate, and lastly at 80°C dried in an oven. The inorganic ion exchanger's different ratios were analyzed and presented in Table 1. Depending on a higher IEC (ion exchange capacity) sample, for further studies S-2 was selected.

2.3. PCz-Sn(IV)phosphate nanocomposite ion exchanger synthesis

The nanocomposite ion exchangers PCz-Sn(IV)phosphate were formulated by carbazole's in-situ oxidative polymerization in the nanosized Sn(IV)phosphate (0.5, 1.0, 1.5, and 2.0 wt.%) presence using $FeCl_3$ as oxidizing agents. The Sn(IV)phosphate different solutions in chloroform were stirred up to 1 hour and fixed solutions of carbazole prepared in chloroform were dropwise added. These solutions were continuously stirred for 1 h and after that fixed amount of $FeCl_3$ (in 50 mL chloroform) was added for a 48 h period with constant stirring. The solution's cream color was transformed to dark green color. The prepared nanocomposite ion exchangers were washed with chloroform to remove impurities. The prepared nanocomposite ion exchangers were dried in an oven at 50°C as well as grounded to fine powders. Table 2 represents nanocomposite ion exchangers' preparation and electrical conductivity.

2.4. Sorption studies

Metal ion selectivity is primarily dependent on metal ion transport behaviour. The balance is more comfortably expressed as regards the distribution coefficients of counter-ions in some practical applications.

With several metal ions' distribution coefficients (K_d values) on PCz-Sn(IV)phosphate composite, batch approaches were employed to obtain 100 mg of exchanger beads in an Erlenmeyer flask with several metal nitrate solutions. 20 mL each in the desired mediums. Further, for 24 h continuous stirring is provided to these solutions. Also, before and after equilibrium, metal ions' concentrations in the solution can be established through titrating against the standard EDTA 0.005 M solution [25] (Table 3).

The metal ion concentration ratio in the exchanger phase as well as the solution phases gives the quantity for distribution, or, the coefficient of distribution; which in a solution is the metal ions' fractional uptake measure opposing H^+ ions through an ion-exchange material as well as following formula is utilized for calculating it mathematically as:

Table 1
Synthesis and IEC of Sn(IV)phosphate ion-exchange material

S. No.	0.1 M Stannic chloride (1 M HCl) (mL)	0.1 M Orthophosphoric acid (mL)	pH	IEC (Meq g^{-1})
S-1	50	100	1	2.0
S-2	***50***	***50***	***1***	***2.1***
S-3	50	150	1	1.4

$$K_d = \frac{(I-F)}{F} \times \frac{V}{M}\left(\text{mL g}^{-1}\right) \quad (1)$$

where I represents metal ion's initial amount in aqueous phases, F represents the metal ion amount in the aqueous phases, V represents the solution volume (mL) and M represents the nanocomposite cation exchanger amount (g).

2.5. Synthesis of PCz-Sn(IV)phosphate nanocomposite ion exchanger membrane

PCz-Sn(IV)phosphate nanocomposite's ion-exchange membrane was developed through approach described in our earlier studies [26]. Composite's distinctive amounts transformed into fine powder as well as combined completely with a calculated polyvinyl chloride (PVC) amount were dissolved in THF for at least 24 h; for finding the optimal membrane compositions which can be used for further studies [27]. PCz-Sn(IV)phosphate composite materials were consequently placed onto pure glass plate, spread in PVC solution, and then maintained in room temperature for 48 h, so that THF could completely evaporate. The resulting membranes were carefully removed from glass plate and washed at room temperature with DMW, on both sides, and the composite ion exchanger membrane.

To evaluate the IEC of PCz-Sn(IV)phosphate, in a beaker, they took 1 M $NaNO_3$ solution as well as H^+ form chose membrane was immersed in it for 24 h. Afterwards, effluent taken out as well as then utilizing a phenolphthalein indicator, standard (0.1 M) NaOH solution is utilized for titrating. Table 4 represents preparation conditions as well as PCz-Sn(IV)phosphate nanocomposite ion-exchange membrane IEC.

2.6. Nanocomposite ion-exchange membrane characterization

Several instrumentation methods are used for characterizing the membrane. The elemental analysis was done by EDX. The thermal behavior was studied by TGA. The membrane's surface morphology was examined with SEM microscopy. The FTIR spectroscopy is utilized for identifying various functional groups within the membrane. "PW 1148/89-based diffractometer with CuKα radiations" is utilized for determining the degree of crystallinity and molecular structure. Membrane's physiochemical characters

Table 2
Synthesis, IEC and conductivity of PCz-Sn(IV)phosphate nanocomposite cation exchanger

S. No.	Sn(IV)phosphate inorganic ion exchanger (chloroform) (g)	Carbazole (chloroform) (g)	$FeCl_3$ (chloroform) (g)	IEC (meq/g)
1	0.5	5	5	1.45
2	***1***	***5***	***5***	***1.60***
3	1.5	5	5	1.75
4	***2***	***5***	***5***	***1.95***
5	2.5	5	5	1.80

Table 3
K_d-values of some metal ions on PCz-Sn(IV)phosphate composite in different solvent systems

Metal ions \ Solvents	0.1 M HNO_3	0.01 M HNO_3	0.001 M HNO_3	0.1 M H_2SO_4	0.01 M H_2SO_4	0.001 M H_2SO_4	0.1 M HCl	0.01 M HCl	0.001 M HCl	DMW
Cu^{2+}	***1,005***	***410***	***2,015***	***1,135***	***1,965***	***1,245***	***1,965***	***920***	***1,015***	***1,495***
Ni^{2+}	545	505	365	960	705	585	565	1,005	495	795
Pb^{2+}	815	1,120	1,135	840	910	1,195	1,165	865	745	1,060
Hg^{2+}	415	265	605	402	405	315	260	295	280	290
Ba^{2+}	845	1,535	1,025	1,085	905	1,065	745	765	840	765
Cd^{2+}	805	695	915	880	615	690	765	485	520	565

Table 4
Condition of preparation and IEC of PCz-Sn(IV)phosphate ion-exchange membrane

S. No.	Composites (g)	Binder		Stirring time (h)	IEC of membrane (Meq g^{-1})
		Polyvinyl chloride (PVC) (g)	THF (mL)		
1	0.25	0.2	25	48	0.59
2	0.50	0.2	25	48	0.42
3	***0.75***	***0.2***	***25***	***48***	***0.81***
4	1.0	0.2	25	48	0.68

which includes thickness, swelling, water content, and porosity were also concluded as mentioned in Table 5.

2.7. Ion-selective membrane electrode and its parameters

The membrane disc is cut out and joined to the glass tube's end, which contains the reference electrode connected to a potentiometer. The electrodes were immersed in a solution of Cu^{2+} with an external reference electrode and a membrane electrode. Two electrodes' potential difference calculates the Cu^{2+} ions activity which in turn is related to its concentration. Standard solutions of Cu^{2+} of known concentration were developed as well as their potential were calculated. Lastly, a concentration vs. potential graph was plotted as well as unknown solution's concentration was measured by utilizing corresponding potential values.

Internal reference electrode (SCE)	Internal electrolyte 0.1 M Cu^{2+}	Ion-exchange Membrane	Sample solution	External reference electrode (SCE)

Following parameters were evaluated to study the characteristics of the electrode:

- Detection limit
- Response time
- Selectivity coefficient
- Linear response range
- Working pH range

In electrode potential (at 25°C ± 2°C) terms, the electrode response, consistent with 0.1 M $Cu(NO_3)_2$ (10^{-10}–10^{-1} M) standard solutions series concentrations, was calculated at "IUPAC Commission for Analytical Nomenclature" described constant ionic strength [28]. A plot of potential measurements of the ion-exchange membrane vs the respective ions selected ion concentration utilizing the electrode assembly in an aqueous medium was analyzed and for checking the system's reproducibility, calibration graphs were plotted 3 times. Response time is described as "the time interval needed for cell potential to become equal to its steady-state or limiting value when the activity of the ion of interest in solution is changed in contact with ISE and reference electrode" [29]. The response time was measured by electrode immersion in the Cu^{2+} ions' 1×10^{-2} M solution as well as instantly shifting to same ion's other solution (10 fold high concentration). The solution potential measured at zero seconds as well as then measured at 5s intervals. After that a graph is plotted for potential vs. time. For calculating the electrode's working pH range, $Cu(NO_3)_2$ (1×10^{-2} M) solution with pH 1 to 10 were prepared as well as then at every pH electrode potential is measured. A electrode potential vs. pH graph was plotted. Further with NaOH and dilute HCl addition resulted in pH variations.

The potentiometric selectivity coefficients (K_{AB}^{POT}) were stated through combining Nicolsky–Eisenman equation dependent solution method: [30]

$$E = \text{constant} + \left(\frac{RT}{z_A F}\right) \ln\left\{a_A + \sum_{B \neq A}^{B} K_{A,B}^{\text{pot}} \left(a_A\right)^{z_A/z_B}\right\} \quad (2)$$

Potentiometric selectivity coefficient describes the ion-selective electrode abilities for distinguishing a specific ion, that is, primary ion from others (interfering ions). The coefficient of selectivity was measured utilizing the given equation as:

$$K_{A,B}^{POT} = \frac{a_A}{\left(a_B\right)_{z_A/z_B}} \quad (3)$$

where $a_A a_B$ and are a primary as well as interfering ion activity respectively; z_A, z_B represents charged on the primary as well as interfering ions. For primary ion, the K_{AB}^{POT} small value indicates a higher preference. This membrane electrode's analytical utility was developed through using it as an indicator electrode in 1×10^{-2} M $Cu(NO_3)_2$ potentiometric titration solution against an EDTA as a titrant. Further a complex is formed when Cu^{2+} ions and EDTA reacts with one another. The sample's ion concentration is measured from the EDTA volume utilized in titration. Further, a graph is plotted between potential values vs. utilized EDTA volume.

3. Result and discussion

In-situ polymerization helps in preparing PCz-Sn(IV) phosphate nanocomposite ion exchanger. For Na^+ the PCz-Sn(IV)phosphate nanocomposite ion exchanger possessed

Table 5
Percent composition of PCz-Sn(IV)phosphate composite ion-exchange membrane

S. No.	Elements	Percentage %	
		PCz-Sn(IV)phosphate ion-exchange membrane	Cu^{2+} adsorbed PCz-Sn(IV)phosphate ion-exchange membrane
1	C	33.45	32.67
2	N	15.32	16.71
3	O	13.52	12.41
4	Fe	0.23	1.04
5	Sn	26.12	25.64
6	P	10.41	09.23
7	Cu	0.00	2.13

the highest IEC that is discovered in 1.95 meq g^{-1} under similar conditions as presented in Table 2. This has been clearly indicated by results that the IEC increases with the number of inorganic groups incorporated in the polymer chain, after the composite formation, there is increase in IEC wherein there exists more exchangeable sites.

In order to understand the capability of the substance to isolate metal ions, we carried out distribution experiments for metal ions in different solvent systems. The results shown in Table 3 point to different K_d-values depending on the solvent structure and composition. In some solvent systems and specifically in DMW K_d-values show that there is strong adsorption whereas Ni^{2+}, Hg^{2+}, Cd^{2+}, Ca^{2+}, and Ba^{2+} show comparatively low adsorption on composite ion-exchange material's surface. The cation-exchanger's ion-selective and adsorption characteristics as well as ion-exchange properties are demonstrated by certain metal ions' high uptake. The metal-exchanger complexes' stability constant is the key deciding factor for the difference shown in the adsorption in different solvents. Different material amounts along with fixed binder amount (200 mg PVC) is utilized for preparing some samples of PCz-Sn(IV)phosphate nanocomposite ion-exchange membranes as well as further "thickness, cracks, materials distribution, surface uniformity, mechanical stability, etc." are measured. For Na^{+} the highest IEC PCz-Sn(IV) phosphate nanocomposite ion-exchange membranes were discovered to be 0.81 meq g^{-1}. Table 4 provides condition of preparation and calculation of IEC of PCz-Sn(IV) phosphate nanocomposite ion-exchange membrane.

Fig. 1a presents the Cu^{2+} absorbed PCz-Sn(IV)phosphate and PCz-Sn(IV)phosphate composite ion-exchange membrane's SEM images. Furthermore, it has been discovered that prepared polymeric composite ion-exchange membrane having porous nature as well as still has denser morphology. Further, Fig. 1b represents Cu^{2+} clear absorption in PCz-Sn(IV)phosphate composite membrane's pores.

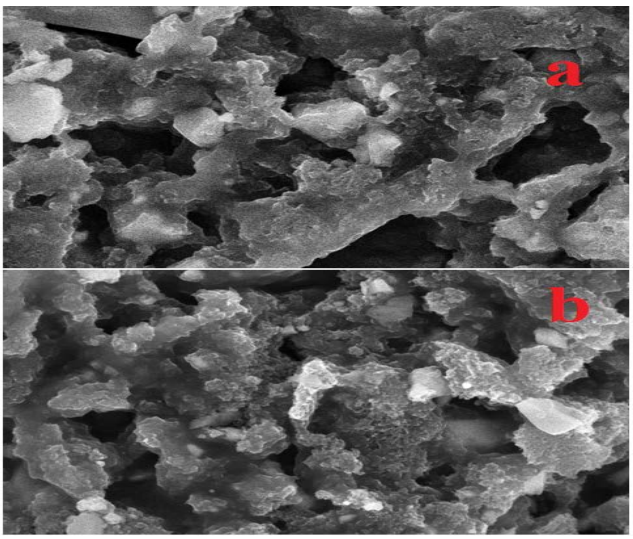

Fig. 1. SEM images of (a) PCz-Sn(IV)phosphate nanocomposite membrane and (b) Cu(II) adsorbed PCz-Sn(IV)phosphate nanocomposite membrane.

Also, elements like Cu, P, Sn, Fe, O, N, and C are presented in Cu^{2+} absorbed PCz-Sn(IV)phosphate and PCz-Sn(IV)phosphate composite ion-exchange membranes, as well as in the ion-exchange membrane these elements' percentage composition were verified from Table 5 as well as is shown in Fig. 2. Fig. 3 presents the PCz-Sn(IV)phosphate FTIR spectra that are immersed in ion solution of Cu(II). In PCz-Sn(IV)phosphate absorption peaks at 1,472 cm^{-1} represents the PCz benzenoid ring's C=C stretching, at 1,623 cm^{-1} is because of quinoid rings 'mode C=C stretching and FTIR spectra at 3,408 cm^{-1} there exists some strong band that indicates –NH stretching frequency. C–N stretching mode causes the peaks at 1,281 and 1,204 cm^{-1} as well as generally at 1,029 cm^{-1} allocated to 4 substituted benzenoid rings, C–H of 1 out-of-plane bending vibration that confirms the PCz formation. The PCz-Sn(IV)phosphate nanocomposite FTIR spectra dipped in Cu(II) ion solution at 3,302 cm^{-1} indicates a strong association that is acquired by –NH stretching frequencies, the absorption peaks at 1,601 cm^{-1} is because of quinoid rings' mode C=C stretching as well as 1,456 cm^{-1} represents the polycarbazole benzenoid ring's C=C stretching which also shows that carbazole polymerization is attained successfully on Sn(IV)phosphate particles' surface, where copper nitrate resulted in a peak at 1,183 cm^{-1}. And broadband between 902 and 738 cm^{-1} with a peak of intensity is because of ionic phosphate group's presence while M–O bonding attributes to peak at 753 cm^{-1} as well as in PCz-Sn(IV)phosphate composite ion-exchange membrane's case 1,029 and 692 cm^{-1} with a peak of intensity is caused by ionic phosphate group presence while M–O bonding attributes to peak at 763 cm^{-1}. Assemblies of peaks at 756–534 cm^{-1} were shifted to 714–483 cm^{-1} [31]. The peaks observed in the PCz-Sn(IV)phosphate nanocomposite membrane dipped in Cu(II) ion solution show a shift in frequencies as compared to the PCz-Sn(IV)phosphate nanocomposite membrane which shows that there has been interaction with a component of nanocomposite ion-exchange material.

Based on the results of EDX and FTIR, formation of PCz-Sn(IV)phosphate ion-exchange membrane's schematic representation is presented by Fig. 4a and b. From scheme 1, in step, I, the monomer of carbazole is oxidized to radical cation through $FeCl_3$ use as an oxidant through one electron removal for forming radical cations. Dimers are formed by oxidative-aromatization reactions as compared to monomers since dimers have more conjugation, and as such, they can be easily oxidized as well as being immediately oxidized to cations until the monomers are all consumed, it continues for advance olymerization reaction. It resulted in production of polycarbazole. Polycarbazole oxidation in an aqueous solution using $FeCl_3$ is followed by polycarbazole binding to Sn(IV)phosphate matrix provided in steps II and III. In Scheme 2, ion-exchange membrane that were adsorbed in Cu(II) metal ion having interaction with PCz-Sn(IV)phosphate and formed PCz-Sn(IV)phosphate ion-exchange membrane which is Cu(II)adsorbed.

The TGA curves in Fig. 5 indicate different weight loss. Upto 200°C~5% weight loss has been indicated by the TGA curve in PCz-Sn(IV)phosphate ion-exchange membrane that might be attributed for water molecules removal as well as later at 300°C~37% membrane decomposition takes place. Further, up to 450°C~6% steady

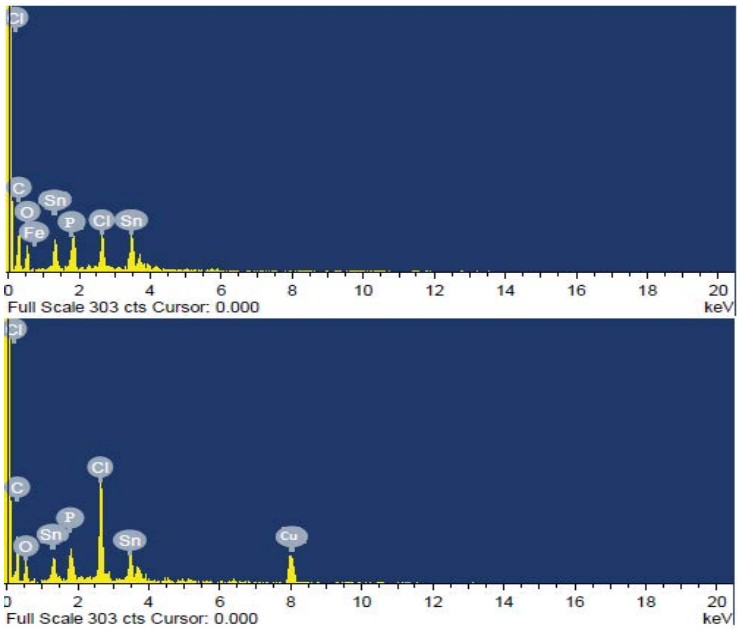

Fig. 2. EDX images of (a) PCz-Sn(IV)phosphate nanocomposite membrane (as prepared) and (b) Cu(II) adsorbed composite membrane.

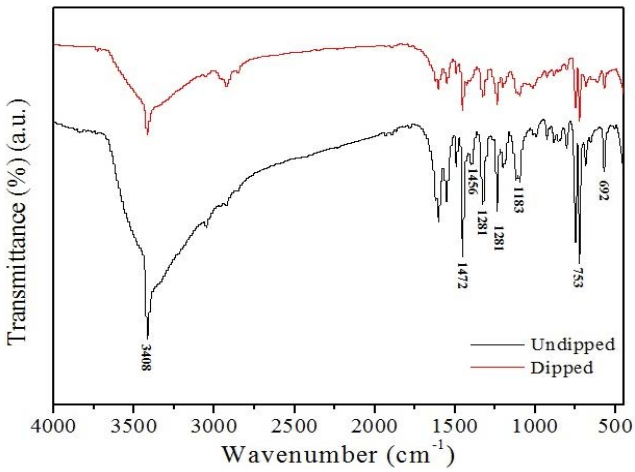

Fig. 3. FTIR photographs of PCz-Sn(IV)phosphate nanocomposite membrane and Cu(II) adsorbed composite membrane.

weight loss was noticed, also up to 500°C~7% weight loss was noticed as well as up to 550°C~5% weight loss was noticed. Further, TGA results clearly indicated that stable up to 650°C PCz-Sn(IV)phosphate ion-exchange membrane is stable thermally. The TGA curves for Cu(II) adsorbed PCz-Sn(IV)phosphate ion-exchange membrane up to 200°C~3% weight loss was indicated by TGA curve resulted by water molecule as well as later at 300°C~42% membrane decomposition is noticed. Similar to the former case up to 450°C~2% steady weight loss was discovered, also, up to 500°C~3% weight loss was noticed as well as ~10% weight loss was observed up to 550°C TGA graph shows that up to 650°C, Cu(II) adsorbed PCz-Sn(IV) phosphate ion-exchange membrane is stable thermally.

The PCz-Sn(IV)phosphate (as prepared) and Cu(II) adsorbed PCz-Sn(IV)phosphate ion-exchange membrane X-ray diffraction (XRD) investigations were performed by utilizing "Rigaku X-ray powder diffractometer with Cu anode (Kα λ = 1.54186 Å) at 30Kv in the $20° \le 2\theta \le 80°$ range. Fig. 6 at room temperature indicates the ion-exchange membrane's typical XRD patterns. PCz-Sn(IV) phosphate (as prepared) ion-exchange membrane's XRD pattern clearly shows that the membrane is amorphous as in the pattern, there does not exist any sharp peak as well as Cu(II) adsorbed PCz-Sn(IV)phosphate ion-exchange membrane shows a peak at 25° that indicate the presence of Cu(II) ions [32]. The ion-exchange membrane's physicochemical characterizations are necessary to be studied before employing it as an "ion-selective electrode". Hence, properties which includes "water content capacities, porosity, thickness, and swelling" are listed in Table 6. For making ion-selective electrode, out of PCz-Sn(IV) phosphate nanocomposite ion-exchange membranes with thickness 0.23, 0.18, 0.16, 0.20 mm respectively, the ion-exchange membrane of thickness 0.16 was chosen. Therefore, these membranes' "less thickness, porosity, swelling, and low water content" suggested that there exist negligible interstices as well as diffusion across membranes are caused through the exchanger site. The ion-selective electrode selectivity and sensitivity is dependent on electro-active material nature. When such materials' nanocomposite ion-exchange membrane is situated among same nature's 2 electrolyte solutions, though having metal ions' varying concentrations, there is predominated phenomenon of ion exchange diffusion. The H^+ ions on membrane surface exchange selectively with metal ions [Cu^{2+}] on nanocomposite ion-exchange membrane, so an electrical potential difference is generated on the membrane. Fig. S1 presents the nanocomposite ion-exchange

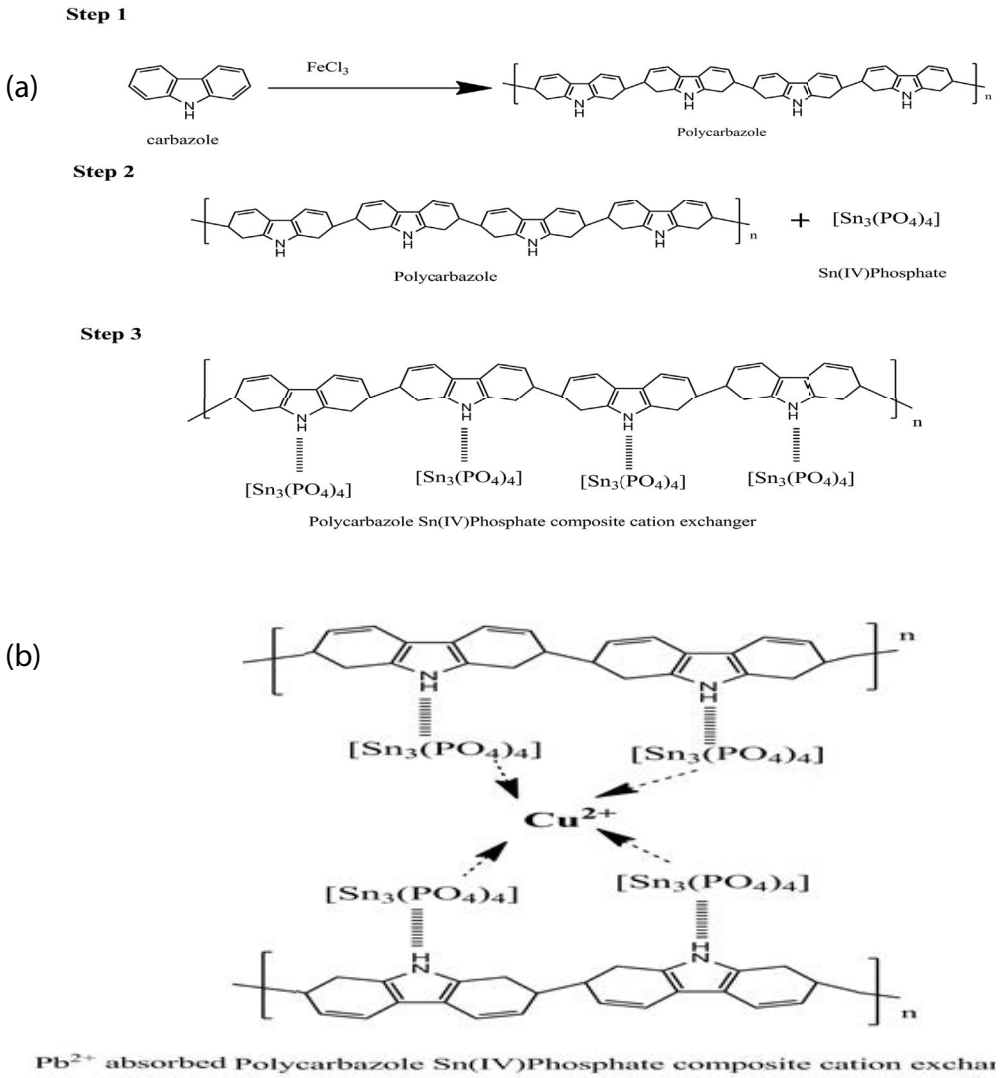

Fig. 4. Schematic representation of (a) the formation of PCz-Sn(IV)phosphate ion-exchange membrane and (b) Cu(II) absorbed PCz-Sn(IV)phosphate composite membrane.

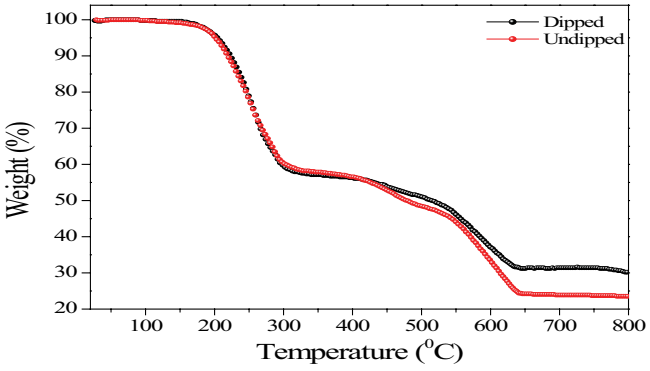

Fig. 5. TGA image of PCz-Sn(IV)phosphate nanocomposite membrane and Cu(II) adsorbed composite membrane.

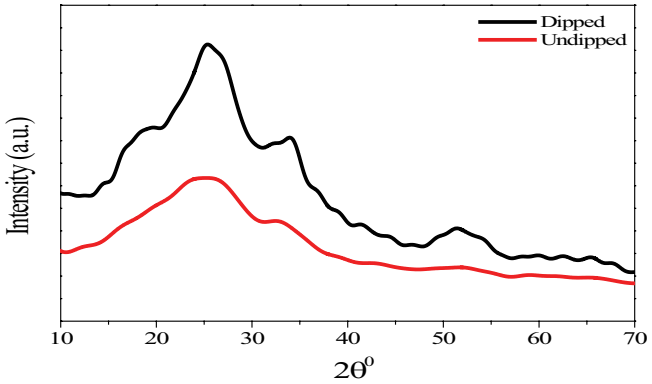

Fig. 6. XRD photographs of PCz-Sn(IV)phosphate nanocomposite membrane and Cu(II) adsorbed composite membrane.

membrane electrode responded to Potentiometric through a broader concentration range of 1×10^{-10} M to 1×10^{-1} M. Further, in 1×10^{-7} M to 1×10^{-1} M range a linear response is showed by PCz-Sn(IV)phosphate electrode. Therefore, the ion-exchange membrane's working concentration range for Cu^{2+} is $\times 10^{-7}$M to 1×10^{-1} M with a 28.25 mV Nerstian

Table 6
Physiochemical characterizations of PCz-Sn(IV)phosphate ion-exchange membrane

S. No.	Thickness of the membrane (mm)	Porosity	Water content as % weight of wet membrane	Swelling
1	0.23	0.0445	0.2136	0.058
2	0.18	0.0580	0.2942	0.067
3	***0.16***	***0.0305***	***0.1065***	***0.031***
4	0.20	0.0485	0.3362	0.048

Table 7
Selectivity coefficient of various interfering ions for Pb^{2+} selective PCz-Sn(IV)phosphate composite cation exchanger membrane

Interfering ions (M^{n+})	Selectivity coefficients (K_{MSM})
Cu^{2+}	1
Ni^{2+}	1.17×10^{-1}
Pb^{2+}	1.3×10^{-1}
Hg^{2+}	2.3×10^{-1}
Cd^{2+}	2.8×10^{-1}
Ba^{2+}	2.9×10^{-1}
Mg^{+2}	1.96×10^{-1}

slope/decade concentrations changes. The pH influence on electrode's potential response was calculated for Cu^{2+} ions' fixed (1×10^{-2}) concentration in various pH value. The 5.0–8.0 pH range for the electrode was evident (as seen in Fig. S2) as the operating pH range for the electrode is known. An sudden transition over pH 8 is due to the Cu^{2+} ions such as $Cu(OH)_2$ precipitation. The ion-selective electrode's response time is another significant element. The average response time is described as "time required for the electrode to reach a stable potential after successive immersion of the electrode in different ion solutions, each having a 10-fold difference in concentration". The response time was measured in 1×10^{-2} Cu^{2+} ion solution contact was measured and Fig. S3 shows the results. Figure clearly showed that PCz-Sn(IV)phosphate electrode response time is 20s. It has also been found that up to 12 months with no significant potential variation at times of which the potential pitch can be reproduced within a maximum of ±1 mV per concentration decade, can be successfully used. Where a potential difference is found in the membrane, 0.1 M $Cu(NO_3)_2$ solutions are re-balanced for 3–4 d. The ion-selective electrodes' most significant characteristic is selectivity behavior which determines possibility of target sample's reliable measurement. MSM (mixed solution method) was utilized fir its determination. Table 7 clearly shows that majority interfering ions exhibit low selectivity coefficient values, which indicates that PCz-Sn(IV) phosphate membrane electrode assembly's performance is not affected. The membrane's strong affinity towards the Cu^{2+} reflected this extraordinary selectivity over other ions. The Cu^{2+} selectivity means it was used as a selective Cu^{2+} indicator electrode with the EDTA solution titrant for the titration of a selective Cu^{2+}. Adding EDTA reduces the potential due to the decrease of the concentration of free metal ions that is Cu^{2+} because of its complication with EDTA Fig. S4. A sharp equivalence point will reliably measure the sum of Cu^{2+} in a solution which is evident from resultant neat titration curve. In this study, the analytical and practical utility of a nanocomposite membrane electrode designed for cation exchange was determined. Fig. S5 is a graph of transport number vs. concentration that relates to the electrode's performance at 1×10^{-9} M to 1×10^{-1} M concentration range.

4. Conclusion

Ion exchangers based on PCz-Sn(IV)phosphate nanocomposite materials are mechanically and thermally stable and exhibit a excellent exchange capacity (1.95 meq g^{-1}). It was found that the material was selective for Cu^{2+}. The heterogeneous ion-exchange membrane was developed by solution casting method using nanocompsite ion exchanger. The PCz-Sn(IV)phosphate and Cu^{2+} absorbed PCz-Sn(IV)phosphate composite ion-exchange membranes were characterized by SEM with EDX, FTIR, TGA and XRD. It is stated that the Cu^{2+} selective electrode showed a linear response from 1×10^{-7} M to 1×10^{-1} M with a pH range of 5–8 and a response time of 20 s. The electrode was successfully used as an indicator in Cu^{2+} ion titrations.

Disclosure of potential conflicts of interests

The authors declare no potential conflicts of interests.

Acknowledgment

This project was funded by the Deanship of Scientific Research (DSR), King Abdulaziz University, Jeddah, Saudi Arabia under grant no. (KEP-34-130-40). The authors, therefore, acknowledge with thanks DSR technical and financial support.

References

[1] A.A. Khan, S. Shaheen, Synthesis and characterization of a novel hybrid nanocomposite cation exchanger poly-o-toluidine Sn(IV) tungstate: its analytical applications as ion-selective electrode, Solid State Sci., 16 (2013) 158–167.
[2] Y. Tanaka, Ion-exchange membrane electrodialysis for saline water desalination and its application to seawater concentration, Ind. Eng. Chem. Res., 50 (2011) 7494–7503.
[3] P. Barbaro, F. Liguori, Ion exchange resins: catalyst recovery and recycle, Chem. Rev., 109 (2008) 515–529.
[4] C.E. Harland, R.W. Grimshaw, Ion Exchange: Theory and Practice, Royal Society of Chemistry, Cambridge, 1994.
[5] P. Raizada, V. Soni, A. Kumar, P. Singh, A.A.P. Khan, A.M. Asiri, V.K. Thakur, V.H. Nguyen, Surface defect engineering of

metal oxides photocatalyst for energy application and water treatment, J. Mater., 7 (2021) 388–418.
[6] M.O. Ansari, F. Mohammad, Thermal stability of HCl-doped-polyaniline and TiO_2 nanoparticles-based nanocomposites, J. Appl. Polym. Sci., 124 (2012) 4433–4442.
[7] C.R. Vestal, Z.J. Zhang, Effects of surface coordination chemistry on the magnetic properties of $MnFe_2O_4$ spinel ferrite nanoparticles, J. Am. Chem. Soc., 125 (2003) 9828–9833.
[8] A.A. Khan, S. Shaheen, Preparations and characterizations of poly-*o*-toluidine/multiwalled carbon nanotubes/Sn(IV) tungstate composite ion exchange thin films and their application as a Pb(II) selective electrode, RSC Adv., 4 (2014) 23456–23463.
[9] A.A. Khan, S. Shaheen, Chronopotentiometric and electroanalytical studies of Ni(II) selective polyaniline Zr(IV) molybdophosphate ion-exchange membrane electrode, J. Electroanal. Chem., 714–715 (2014) 38–44.
[10] A.A. Khan, R. Ahmad, M. Zeeshan, S. Shaheen, Synthesis, characterization, electrical and dielectrical studies of polypyrrole-Sn(IV)arsenotungstate nanocomposite ion-exchange membrane: its selectivity as Ba(II), J. Mol. Liq., 221 (2016) 999–1007.
[11] L. Mathiasson, Membrane extraction in analytical chemistry, J. Sep. Sci., 24 (2001) 495–507.
[12] W.J. Koros, G.K. Fleming, Membrane-based gas separation, J. Membr. Sci., 83 (1993) 1–80.
[13] Y. Chen, Y. Luo, Precisely defined heterogeneous conducting polymer nanowire arrays – fabrication and chemical sensing applications, Adv. Mater., 21 (2009) 2040–2044.
[14] N.K. Guimard, N. Gomez, C.E. Schmidt, Conducting polymers in biomedical engineering, Prog. Polym. Sci., 32 (2007) 876–921.
[15] H. Zou, S. Wu, J. Shen, Polymer/silica nanocomposites: preparation, characterization, properties, and applications, Chem. Rev., 108 (2008) 3893–3957.
[16] D.W. Hatchett, M. Josowicz, Composites of intrinsically conducting polymers as sensing nanomaterials, Chem. Rev., 108 (2008) 746–769.
[17] A.A.P. Khan, A. Khan, M.M. Rahman, A.M. Asiri, M. Oves, Chemical sensor development and antibacterial activities based on polyaniline/gemini surfactants for environmental safety, J. Polym. Environ., 26 (2018) 1673–1684.
[18] A.A.P. Khan, A. Khan, M.M. Rahman, A.M. Asiri, Conventional surfactant-doped poly (o-anisidine)/GO nanocomposites for benzaldehyde chemical sensor development, J. Sol-Gel Sci. Technol., 77 (2016) 361–370.
[19] A.A.P. Khan, A. Khan, M.M. Rahman, A.M. Asiri, M. Oves, Lead sensors development and antimicrobial activities based on graphene oxide/carbon nanotube/poly(*o*-toluidine) nanocomposite, Int. J. Biol. Macromol., 89 (2016) 198–205.
[20] A.A.P. Khan, A. Khan, M.A. Alam, M. Oves, A.M. Asiri, M.M. Rahman, Inamuddin, Chemical sensing platform for the Zn^{+2} ions based on poly(o-anisidine-co-methyl anthranilate) copolymer composites and their environmental remediation in real samples, Environ. Sci. Pollut. Res., 25 (2018) 27899–27911.
[21] A. Khan, A.A.P. Khan, A.M. Asiri, M.M. Rahman, B.G. Alhogbi, Preparation and properties of novel sol-gelderived quaternized poly(n-methyl pyrrole)/Sn(II)SiO3/CNT composites, J. Solid State Electrochem., 19 (2015) 1479–1489.
[22] M. Zeeshan, R. Ahmad, A.A. Khan, A.A.P. Khan, G.C. Bazan, B.G. Alhogbi, H.M. Marwani, S. Singh, Fabrication of a lead ion selective membrane based on a polycarbazole Sn(IV) arsenotungstate nanocomposite and its ion-exchange membrane (IEM) kinetic studies, RSC Adv., **11 (**2021) 4210–4220.
[23] M. Zeeshan, R. Ahmad, A.A.P. Khan, A.A. Khan, S. Singh, Potentiometric titration studies of poly(aniline-co-pyrrole)-Sn(IV)tungstoarsenate composite cation-exchange membrane and their application as a Ni(II) selective electrode, J. Dispersion Sci. Technol., 8 (2020) 1192–1200.
[24] C. McHenry, The New Encyclopedia Britannica, 3 (15 ed.), Encyclopedia Britannica, Inc., Chicago, 1992, p. 612, ISBN 0-85229-553-7.
[25] C.N. Reilley, R.W. Schmid, F.S. Sadek, Chelon approach to analysis: I. Survey of theory and application, J. Chem. Educ., 36 (1959) 555–564.
[26] A.A. Khan, M.M. Alam, Synthesis, characterization and analytical applications of a new and novel 'organic–inorganic' composite material as a cation exchanger and Cd(II) ion-selective membrane electrode: polyaniline Sn(IV) tungstoarsenate, React. Funct. Polym., 55 (2003) 277–290.
[27] A. Craggs, G.J. Moody, J.D.R. Thomas, PVC matrix membrane ion-selective electrodes. Construction and laboratory experiments, J. Chem. Educ., 51 (1974) 541, doi: 10.1021/ed051p541.
[28] G.G. Guilbault, Recommendations for Publishing Manuscripts on Ion-Selective Electrodes, Commission on Analytical Nomenclature, Analytical Chemistry Division, IUPAC Standards Online, Ion-Sel. El. Rev., 1 (1969) 139, doi: 10.1515/iupac.53.0052.
[29] C. Maccà, Response time of ion-selective electrodes: current usage versus IUPAC recommendations, Anal. Chim. Acta, 512 (2004) 183–190.
[30] Y. Umezawa, K. Umezawa, H. Sato, Selectivity coefficients for ion-selective electrodes: recommended methods for reporting KA,Bpot values (Technical Report), Pure Appl. Chem., 67 (1995) 507–518.
[31] A. Khan, A.M. Asiri, M.A. Rub, N. Azum, A.A.P. Khan, S.B. Khan, M.M. Rahman, I. Khan, Synthesis, characterization of silver nanoparticle embedded polyaniline tungstophosphate-nanocomposite cation exchanger and its application for heavy metal selective membrane, Compos. Part B, 45 (2013) 1486–1492.
[32] M.K. Amini, M. Mazloum, A.A. Ensafi, Lead selective membrane electrode using cryptand(222) neutral carrier, J. Anal. Chem., 364 (1999) 690–693.

Supplementary information

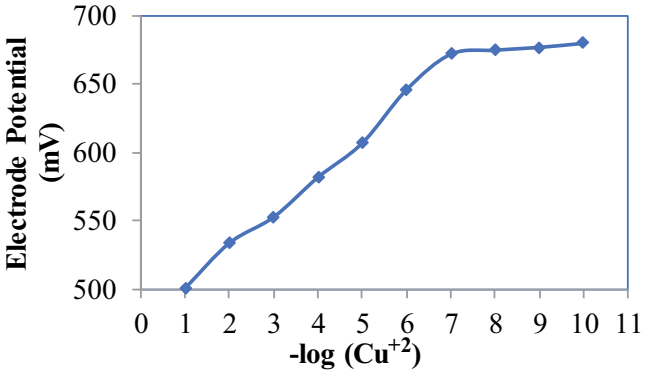

Fig. S1. Calibration curve of PCz-Sn(IV)phosphate nanocomposite membrane electrode in aqueous solution of $Cu(NO_3)_2$.

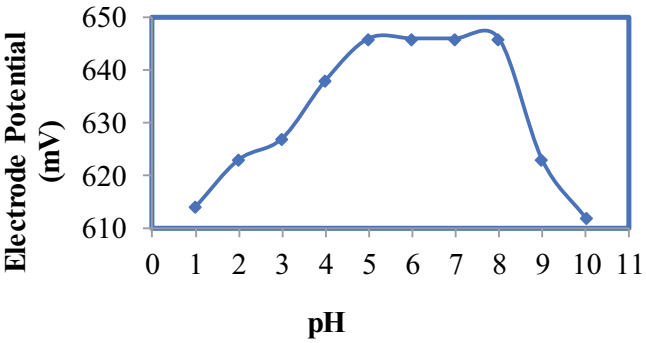

Fig. S2. Effect of pH on the potential response of the PCz-Sn(IV) phosphate nanocomposite membrane electrode.

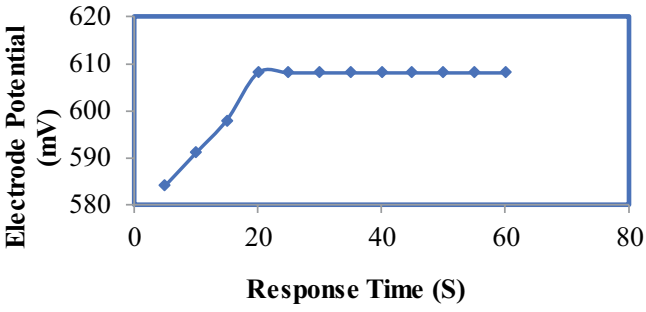

Fig. S3. Plot of transport no. of PCz-Sn(IV)phosphate nanocomposite membrane electrode in aqueous solution of $Cu(NO_3)_2$.

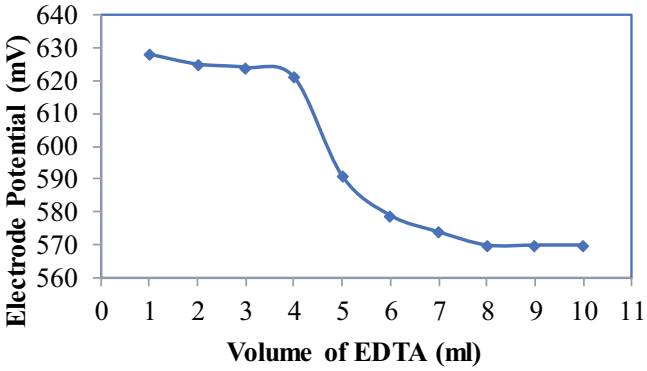

Fig. S4. Potentiometric titration of PCz-Sn(IV)phosphate nanocomposite membrane electrode at 1 × 10^{-2} M Cu(II) concentration.

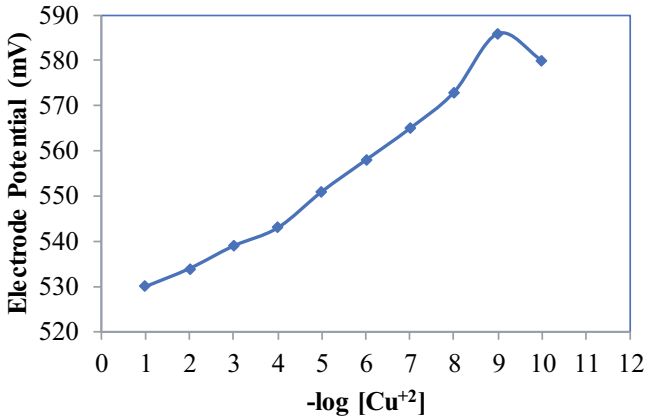

Fig. S5. Plot of transport number of PCz-Sn(IV)phosphate nanocomposite membrane electrode in aqueous solution of $Cu(NO_3)_2$.